Surface Dynamics of Fluidized Beds and Quality of Fluidization

W. J. RICE and R. H. WILHELM

Princeton University, Princeton, New Jersey

Solutions of linearized Navier-Stokes equations have been developed for the motion of arbitrary two-dimensional waves occurring at any interface between the emulsion phase of a fluidized bed and the particle-free, fluid phase. In all cases for which the bed particles are denser than the fluidizing fluid the solutions showed that the lower interface of a bed always is unstable and the upper, stable. The quality of fluidization is suggested to be related at least in part to the rate of growth of surface waves, this rate depending upon physical properties of the system and length of the disturbing wave.

The question of the stability of interfaces between two fluids of different physical properties (density, viscosity, etc.) has attracted considerable interest in recent years (*1, 3, 8*). In this paper the approach is extended by means of the Taylor instability theory (*8*) to the stability of interfaces between the dense bed phase of a fluidized bed and the particle-free fluid phase. In particular, instabilities at the bed entrance are studied as contributors to bed quality through initiation of *bubbles* at this site, and instabilities at the upper surfaces of bubbles are investigated as a mechanism tending to limit bubble growth. By solving linearized Navier-Stokes equations describing the motions of an interface in terms of arbitrary, two dimensional waves for models of fluidized beds, one finds that the lower interface of a bed composed of particles denser than the fluidizing fluid (hereafter called the support fluid) is always unstable and the upper, stable. Unstable interfaces are those on which an imposed disturbance grows in amplitude with time; stable interfaces are those on which a disturbance is damped out.

Taylor's theory, first discussed in 1950, concerns a stability analysis of interfaces between two fluids of different densities when the fluids are accelerated either mechanically or gravitationally in a direction perpendicular to the interface. It was shown by solution of the linearized fluid dynamical equations for systems subject only to gravitational acceleration, with viscosity and surface tension neglected, that, if a horizontal interface at rest under gravity is displaced into the form of small waves, this surface is stable or unstable according to whether the acceleration of gravity is directed from the lighter to the heavier fluid or vice versa. Lewis (*3*) verified these conclusions experimentally for air-water, air-glycerine, and benzene-water interfaces. The experimental phenomena for fluid interfaces photographed by Lewis are suggestive of fluidized-bed behavior. Bellman and Pennington (*1*) made theoretical extensions to include effects of viscosity and surface tension.

When one applies a Taylor type of analysis to fluidized beds, the assumption is made that the system is, as an approximation, composed of two distinct fluid phases: the support fluid (liquid or gas) and the dense-phase fluidized bed itself. In a bed there are a number of positions where an interface between two fluids of different physical properties occurs: at the top of the bed, at the bottom support, and at slugs, bubbles, or other discontinuities that rise through the bed. Figure 1 shows an idealized general view of a cross section of a bed containing bubbles.

BED MODELS

A number of idealized and simplified models of the bed will be introduced a this point and will incorporate two types of physical characteristics: the dense-phase intensive properties of density and viscosity and the relative motion of solid particles and the support fluid. These models were selected as mathematically amenable approximations to true behavior of fluidized beds and thus at best only approach actuality. While the emphasis here is directed to the properties of the dense phase, the support-fluid properties of density and viscosity, which are important also, are those associated with a normal fluid. In all models turbulence has been included only in the sense of serving as a possible source of interfacial disturbances. Turbulent motion is not represented directly in equations.

Two basic models have been devised which consider fraction voids in the dense-bed phase to be constant for any given system and flow rate. Local variations in support-fluid velocity, which constitute the direct source of interfacial disturbances, are assumed to occur, producing displacements of the bed particles. It is these displacements appearing at an interface of the bed which constitute the visible interfacial disturbances.

Model 1 uses a fixed-bed approach because it postulates particles remaining more or less in fixed geometrical array. There is movement of particles only as is necessary to accommodate the displacement of interfaces. In coursing through the array the support fluid encounters frictional resistance, and its velocity also is modified. As a convenient but not necessary assumption, density and viscosity of the dense-bed phase and of the support fluid are taken to be the same. The interface is assumed to move so as to maintain a constant slip velocity.

In model 2 the dense bed phase is assumed to be an *emulsion* in which particles tend to follow fluid motions more closely than in model 1, but a constant slip velocity still is maintained. Bed density is taken as a weighted average of solid and support-fluid densities. Bed-phase viscosity is taken at a value considerably greater than that of the support fluid. Bed viscosity may be estimated from experiments on fluidized beds or on hindered settling of particles. Here bed viscosities have been estimated from the work of Matheson, Herbst, and Holt (*5*) and Long (*4*) with rotating spindles in fluidized beds.

A variant of model 2 (model 2*a*) considers the slip velocity to be constant only in the steady flow condition. The interface is considered to move under the influence of changes in the drag force produced by velocity fluctuations; the rate of movement of the interface is determined by acceleration caused by this unbalanced force. Here the drag force is estimated by utilizing Stokes's Law, and so the analysis must be limited to cases of particles sufficiently small for this to be a satisfactory approximation.

THEORY

Transference of the interfacial stability analysis into quantitative terms requires formulation in precise mathematical terms. Theory is clarified by a treatment of the physical picture at the point of introduction into the mathematical development; therefore the essential points involved will be illustrated for one interface of one model. Final expressions for the various other cases are then presented. Details of all derivations are available elsewhere (*7*).

Equations for motion of an interface are basically the same for models 1 and 2 except for the presence of a friction term for the bed phase in model 1. Only the outline of derivation for the lower

W. J. Rice is at Villanova University, Villanova, Pennsylvania.

interface in model 1 will be traced in this section.

A two-dimensional, sinusoidal velocity wave in u and v is imposed at the lower interface of the bed. Associated with this velocity wave is a two-dimensional, sinusoidal, vertical displacement (η) of the interface of identical wave length. Linearized equations of motion and continuity for bed-phase and support-fluid phase are solved in terms of potential functions.

An equation of continuity is

$$\frac{\partial u}{\partial x} + \frac{\partial v}{\partial y} = 0 \tag{1}$$

Equations of motion are

$$\frac{\partial u}{\partial t} + \frac{1}{\rho}\frac{\partial p}{\partial x} = \frac{\mu}{\rho}\left(\frac{\partial^2 u}{\partial x^2} + \frac{\partial^2 u}{\partial y^2}\right) - F_x \tag{2}$$

$$\frac{\partial v}{\partial t} + \frac{1}{\rho}\frac{\partial p}{\partial y} + g = \frac{\mu}{\rho}\left(\frac{\partial^2 v}{\partial x^2} + \frac{\partial^2 v}{\partial y^2}\right) - F_y \tag{3}$$

In accordance with the well-known convenience of fluid mechanics, transformations are made into potential functions ϕ and ψ. These are defined by

$$u = -\frac{\partial \phi}{\partial x} - \frac{\partial \psi}{\partial y} \tag{4}$$

$$v = -\frac{\partial \phi}{\partial y} + \frac{\partial \psi}{\partial x} \tag{5}$$

$$p = p_0 - g\rho y + \rho\frac{\partial \phi}{\partial t} - F_y y \rho \tag{6}$$

with the further restriction

$$\frac{\partial^2 \phi}{\partial x^2} + \frac{\partial^2 \phi}{\partial y^2} = 0 \tag{7}$$

$$\frac{\mu}{\rho}\left(\frac{\partial^2 \psi}{\partial x^2} + \frac{\partial^2 \psi}{\partial y^2}\right) = \frac{\partial \psi}{\partial t} \tag{8}$$

To satisfy these equations for the bed phase, a solution is written in the following equations:

$$\phi_1 = Ae^{-Ky+nt}\cos Kx + My \tag{9}$$

$$\psi_1 = Be^{-m_1 y+nt}\sin Kx \tag{10}$$

$$p_1 = p_{0_1} - g\rho_1 y + \rho_1\frac{\partial \phi}{\partial t} - F_y y \rho_1 \tag{11}$$

where

$$m_1 = +\sqrt{K^2 + \frac{\rho_1 n}{\mu_1}}$$

Similarly for support-fluid phase these equations provide a solution:

$$\phi_2 = Ce^{Ky+nt}\cos Kx + Ny \tag{12}$$

$$\psi_2 = De^{m_2 y+nt}\sin Kx \tag{13}$$

$$p_2 = p_{0_2} - g\rho_2 y + \rho_2\frac{\partial \phi_2}{\partial t} \tag{14}$$

where

$$m_2 = +\sqrt{K^2 + \frac{\rho_2 n}{\mu_2}}$$

With the interfacial position denoted by $\eta(x, t)$, the rate of movement of the interface when one applys the condition of constant slip velocity is given by

$$\frac{\partial \eta}{\partial t} = v_2 - C' \tag{15}$$

Alternately after one employs Equations (5), (12), and (13)

$$\frac{\partial \eta}{\partial t} = Ke^{nt}\cos Kx(-C + D) - N - C' \tag{16}$$

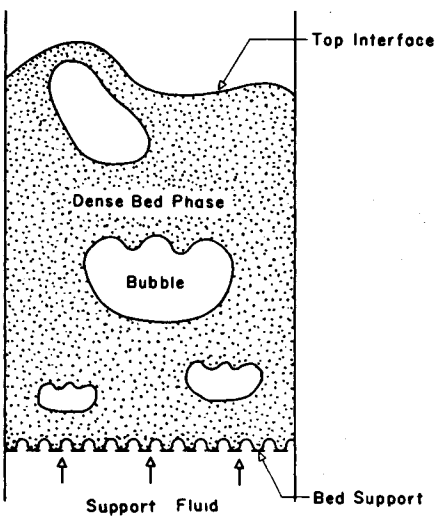

Fig. 1. Cross section of a fluidized bed.

On integration Equation (16) yields

$$\eta = \frac{K(-C + D)\cos Kx}{n}e^{nt} + (-N - C')t + C_1 \tag{17}$$

If interfacial position at time zero is now taken as

$$\eta_0 = \frac{K(-C + D)\cos Kx}{n} \tag{18}$$

then $C_1 = 0$ and $C' = -N$. Therefore

$$\frac{\eta}{\eta_0} = e^{nt} \quad \text{at any} \quad x \tag{19}$$

This important relation shows that the rate of change of amplitude of an interfacial disturbance is proportional to the exponential (nt).

To relate the constant n to the wave length of the surface disturbance as well as to the physical properties of the fluid phases the following interfacial boundary conditions are imposed:

$$u_1 = u_2 \tag{20}$$

$$v_1 = v_2 + \frac{C'(1 - \epsilon)}{\epsilon} \tag{21}$$

$$-p_1 + 2\mu_1\frac{\partial v_1}{\partial y} = -p_2 + 2\mu_2\frac{\partial v_2}{\partial y} \tag{22}$$

$$\mu_1\left(\frac{\partial v_1}{\partial x} + \frac{\partial u_1}{\partial y}\right) = \mu_2\left(\frac{\partial v_2}{\partial x} + \frac{\partial u_2}{\partial y}\right) \tag{23}$$

Equations (20) and (21) result from material balances across the interface and (22) and (23) from equating components of the stress tensor at the interface. On substitution of Equations (9), (10), (12), and (13) into (4), (5), (11), and (14) and then into (20), (21), (22), and (23) these four conditions on the constants A, B, C, and D are secured as follows:

$$KA + m_1 B - KC + m_2 D = 0 \tag{24}$$

$$A + B + C - D = 0 \tag{25}$$

$$\left(-\rho_1 n - 2\mu_1 K^2 + \frac{F_y \rho_1 K}{n}\right)A + \left(-2\mu_1 m_1 K + \frac{F_y \rho_1 K}{n}\right)B + (\rho_2 n + 2\mu_2 K^2)C - 2\mu_2 m_2 K D = 0 \tag{26}$$

$$2\mu_1 K^2 A + \mu_1(K^2 + m_1^2)B + 2\mu_2 K^2 C - \mu_2(K^2 + m_2^2)D = 0 \tag{27}$$

Such equations have nontrivial solutions when the determinant of the coefficients vanishes. The solution in the form of n as a function of K for this case (that is, model 1, lower interface) is

$$[-F_y K\rho_1 + (\rho_1 + \rho_2)n^2][(\mu_1 K + \mu_2 m_2) + (\mu_2 K + \mu_1 m_1)] + 4nK[(\mu_1 K + \mu_2 m_2)(\mu_2 K + \mu_1 m_1)] = 0 \tag{28}$$

When $\mu_1 = \mu_2 = \mu_f$ and $\rho_1 = \rho_2 = \rho_f$, Equation (28) degenerates to

$$[-F_y K\rho_f + 2\rho_f n^2] + 2nK\mu_f(K + m) = 0 \tag{29}$$

where

$$F_y = \frac{(1 - \epsilon)(\rho_s - \rho_f)g}{\rho_f} \text{ [Ref. (9)]} \tag{30}$$

By somewhat similar procedures (7), the following equations are obtained for other cases

Model 1, Upper Interface

$$[F_y K\rho_1 + (\rho_1 + \rho_2)n^2][(\mu_1 K + \mu_2 m_2) + (\mu_2 K + \mu_1 m_1)] + 4nK[(\mu_1 K + \mu_2 m_2)(\mu_2 K + \mu_1 m_1)] = 0 \tag{31}$$

Model 2, Lower Interface

$$[-Kg(\rho_1 - \rho_2) + (\rho_1 + \rho_2)n^2] \cdot [(\mu_1 K + \mu_2 m_2) + (\mu_2 K + \mu_1 m_1)]$$

$$+4nK[(\mu_1K+\mu_2m_2)(\mu_2K+\mu_1m_1)]=0 \quad (32)$$

Model 2, Upper Interface

$$[-Kg(\rho_2-\rho_1)+(\rho_1+\rho_2)n^2]\cdot[(\mu_1K+\mu_2m_2)+(\mu_2K+\mu_1m_1)]+4nK[(\mu_1K+\mu_2m_2)(\mu_2K+\mu_1m_1)]=0 \quad (33)$$

When $\mu_2 \ll \mu_1$ and $\rho_2 \ll \rho_1$, Equation (33) can be simplified to

$$[\rho_1(n^2 + Kg)] + \frac{4\mu_1{}^2m_1K^2}{\rho_1}(m_1 - K) = 0 \quad (34)$$

Model 2a, Lower Interface

$$\left[\frac{H}{G}+(\rho_1+\rho_2)n\right][K(\mu_1+\mu_2)+\mu_1m_1+\mu_2m_2]+K^3\left[\mu_2{}^2\left(1-\frac{1}{G}\right)+\mu_1\mu_2\left(3+\frac{1}{G}\right)\right]+K^2\left[\mu_2{}^2m_2\left(1+\frac{3}{G}\right)+\mu_1\mu_2m_1\left(1-\frac{1}{G}\right)+4\mu_1{}^2m_1\right]+K\left[(\mu_2{}^2m_2{}^2+\mu_1\mu_2m_2{}^2)\left(-1+\frac{1}{G}\right)+2\mu_1\mu_2m_1m_2\left(1+\frac{1}{G}\right)\right]+(\mu_2{}^2m_2{}^3+\mu_1\mu_2m_1m_2{}^2)\left(-1+\frac{1}{G}\right)=0 \quad (35)$$

where

$$G = \frac{1}{\epsilon}\left[\frac{\epsilon + \frac{\rho_v d^2 n}{18\mu_1}}{1 + \frac{\rho_v d^2 n}{18\mu_1}}\right] \quad (36)$$

and

$$H = \frac{-gK(\rho_1 - \rho_2)}{n\left(1 + \frac{\rho_v d^2 n}{18\mu_1}\right)} \quad (37)$$

Model 2a, Upper Interface

$$\left[-\frac{H}{G}+(\rho_1+\rho_2)n\right][K(\mu_1+\mu_2)+\mu_1m_1+\mu_2m_2]+K^3\left[\mu_1{}^2\left(1-\frac{1}{G}\right)+\mu_1\mu_2\left(3+\frac{1}{G}\right)\right]+K^2\left[\mu_1{}^2m_1\left(1+\frac{3}{G}\right)+\mu_1\mu_2m_2\left(1-\frac{1}{G}\right)+4\mu_2{}^2m_2\right]+K\left[\mu_1{}^2m_1{}^2\left(-1+\frac{1}{G}\right)+\mu_1\mu_2m_1{}^2\left(-1+\frac{1}{G}\right)+2\mu_1\mu_2m_1m_2\left(1+\frac{1}{G}\right)\right]+\left[\mu_1{}^2m_1{}^3\left(-1+\frac{1}{G}\right)+\mu_1\mu_2m_1{}^2m_2\left(-1+\frac{1}{G}\right)\right]=0 \quad (38)$$

where G and H are defined by Equations (36) and (37).

Table 1 summarizes the distinctions in the physical properties of the phases used in the equations for the various models.

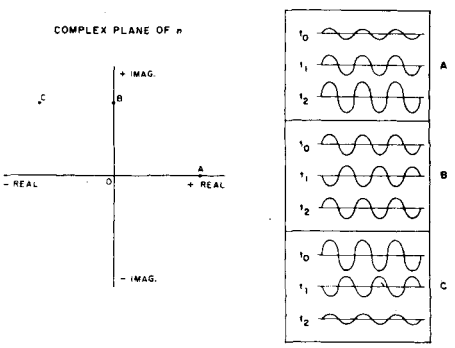

Fig. 2. Significance of n.

TABLE 1

Physical property	Model 1	Model 2 and 2a
ρ_1	ρ_f	$\epsilon\rho_f + (1-\epsilon)\rho_s$
ρ_2	ρ_f	ρ_f
μ_1	μ_f	μ_b
μ_2	μ_f	μ_f
F_y	$\frac{(1-\epsilon)(\rho_s-\rho_f)g}{\rho_f}$	0

Equations (28), (31), (32), (33), (35), and (38) are tenth-order polynomials in n, and Equations (29) [a simplified version of (28)] and (34) [a simplified version of (33)] are of the fourth order. Application of the principle of the argument from complex variables allows determination to be made of the location in the complex n plane of roots which satisfy the physical conditions that were introduced through initial and boundary conditions.

The preceding mathematical development was limited to sinusoidal disturbances of some wave length ($\lambda = 2\pi/K$). However, since the differential equations used were linear, arbitrary disturbances may be expected to be handled by Fourier analysis. Questions of convergence in somewhat similar cases are considered in (*1*).

DISCUSSION

Three aspects of fluidized-bed interfaces deserve special consideration. First, likely sources of interfacial disturbances are commented upon. Second, consideration is given to the physical interpretation of the characteristic n vs. wave-length relations which have been developed, particularly in terms of effect on bubble initiation and bubble stability. Third consideration is given to the relationship between behavior within beds after the bubble initiation has already occurred and the interface is stable.

The analysis to this point has dealt with the problem of how the fluidized-bed system, in particular its interfaces, reacts to disturbances of different wave lengths. The formulation of the problem does not include any statement of how these disturbances may be generated. A number of disturbance sources suggest themselves from the physical arrangements of fluidized beds. Prominently there is the influence of screen or similar bed support which serves to distribute the support fluid at the bed entrance and at the same time imposes a spatially periodic velocity profile at the lower interface. The bed support may introduce some measure of turbulence as a component of disturbance. The support also restricts or prevents net downward motion of particles. The bed support as a contributor to local quality of fluidization has been studied experimentally by Morse and Ballou (*6*) and by Grohse (*2*) using bed capacity and X-ray absorption respectively to measure local particle concentration.

Within the bed one may visualize disturbances that range in wave length from the order of individual particle diameter to that of a full bed, the latter being due to gross circulation patterns. Between these likely limits there may be an almost continuous range of disturbance wave lengths owing to grids, baffles, heat exchanger tubes, thermocouple wells, passage of bubbles or slugs, etc. Observation of fluidized beds suggests that behavior in close vicinity to entrance grids is indeed subject to local disturbance contributions by the grids, whereas interfaces in bubbles, slugs, or at the top of the bed, that is, far removed from the grid, are subject to disturbances characteristic of the bulk of the bed; such interfaces are commonly no longer directly influenced by the grid support.

Turning now to the interpretation of stability analyses as applied to fluidized beds, one can see [Equation (19)] that the amplitude of an interfacial disturbance changes exponentially (as e^{nt}). Furthermore the only allowable root for n at the lower interface of the bed (or upper interface of a bubble) is a positive real number [Equations (28), (29), (32), and (35)]. At the upper interface of the bed (or lower interface of a bubble) the allowable roots of n are a complex con-

jugate pair with negative real parts [Equations (31), (33), (34), and (38)]. These particular locations of roots in the complex n plane signify that the lower bed interface is inherently unstable, the size of n being a direct index of magnitude of instability, whereas the upper bed interface is inherently stable. At the latter position the imaginary part of n indicates oscillatory motion (reminiscent of ocean waves) with frequency $I(n)/2\pi$; the real part represents damping of the oscillation. These matters are summarized in Figure 2 which reviews the significance of the location of n in the complex plane for allowable roots in terms of the time variation of a wave from t_0 to t_1 to t_2. Condition A represents an unstable interface with a nonoscillating wave, B a neutral oscillating interface, and C a stable oscillating interface (that is, with damping).

Unstable Interface

Figures 3 and 4 illustrate typical relations for models 1 and 2 between n and a wave number. The curves were computed to represent diverse gas- and liquid-solid systems known to include different quality characteristics. A maximum value of n appears at some wave length for each system. In their studies of the interface between two normal fluids Bellman and Pennington (*1*) first reported such a characteristic curve, and they called the wave length corresponding to maximum n the *most dangerous* because the amplitude of the wave corresponding to this disturbance grows more rapidly than all others. As shown in Figures 3 and 4 the maximum is quite broad in some cases.

One immediate conclusion that may be drawn from Figures 3 and 4 is independent of the model of fluidization; the ordering of systems by relative values of n, taken at the maxima, is identical with the ordering of visual quality of fluidization as observed in the laboratory of the authors as well as in those of other investigators. The particular systems considered here are lead shot–air, glass beads–air, Aerocat catalyst–air, lead shot–water, glass beads–water, and Socony-Mobil catalyst-beads–water. Similar ordering occurs if comparisons are made at any given wave length rather than at the wave length corresponding to maximum n. Thus as a first approximation experimental quality of fluidization (or bubbling tendency) is linked with mathematical analysis.

The effect of bed viscosity as a variable is isolated in Figure 5. The sole effect of increasing bed viscosity is to reduce the value of n at higher values of K (that is, the smaller wave lengths) without affecting values of n at longer wave lengths. Thus in the viscosity-insensitive, long-wave-length region of the parametric curves, typical numbers might be 10- or 100-cm. wave lengths, corresponding to K values of about 0.6 and 0.06 cm.$^{-1}$, respectively. By contrast it is clear that at short wave lengths viscosity does play an important role in stabilizing the interface.

The various properties of unstable interfaces previously discussed also suggest possible behavior within a fluidized bed as well as at the surface. An instability initiated at an interface may grow and develop into a bubble that rises through the bed. Such a bubble may continue to grow by itself or by chance coalescence with others. If the instability of the system is not large, as in cases known to give particulate fluidization, no recognizable bubbles may develop in the bed. Furthermore the effect of the supporting grid spacing may be explained in terms of the wave length of the primary disturbance produced by the grid. Spacings introducing disturbance wave lengths corresponding to large values of n should tend to lower the quality of fluidization in the vicinity of the grid by more rapidly initiating bubbles, as confirmed by observations (*2*, *6*). With systems of high bed viscosity having extremely poor quality fluidization observations indicate little or no effect of grid spacing. This is consistent with the fact that for such systems the maximum value of n occurs at considerably longer wave lengths than are produced by the usual grid spacings.

On the other hand present analysis may be interpreted as containing elements that act in the direction of reducing bubble size, should it fortuitously become excessive. Large bubbles in gas-solid systems, for example, are observed experimentally to have a raining phenomenon from the roof of the bubble, with pour points at definite position intervals. [See Lewis (*3*) for analogous behavior with a water-air system.] Such tendencies toward bubble destruction through instability at the upper bubble surface may be discussed in terms of viscosity (Figure 5).

Let there be, for convenience, a bubble that is large compared to the wave length of maximum n for its system. It will also be assumed, as before,

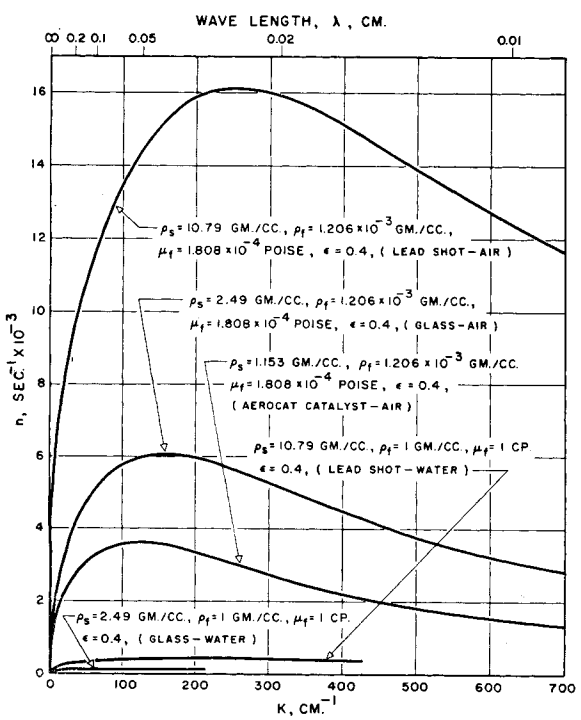

Fig. 3. Typical values of n for model 1, unstable interface.

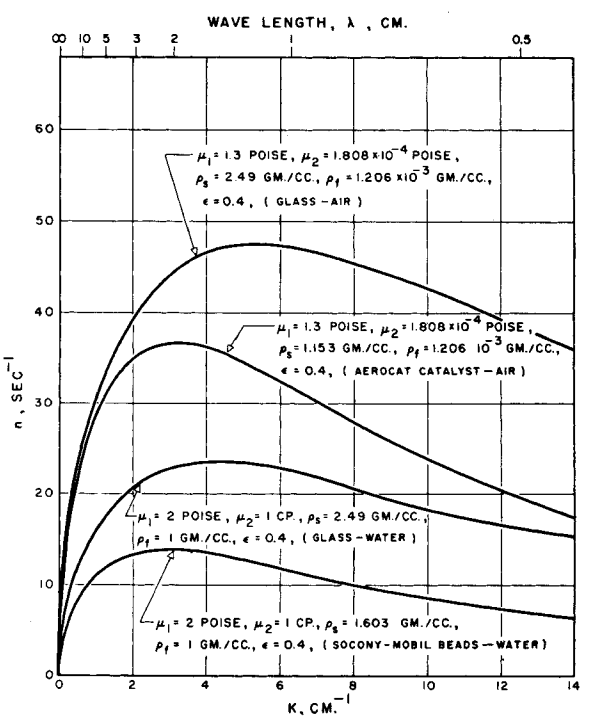

Fig. 4. Typical values of n for model 2, unstable interface.

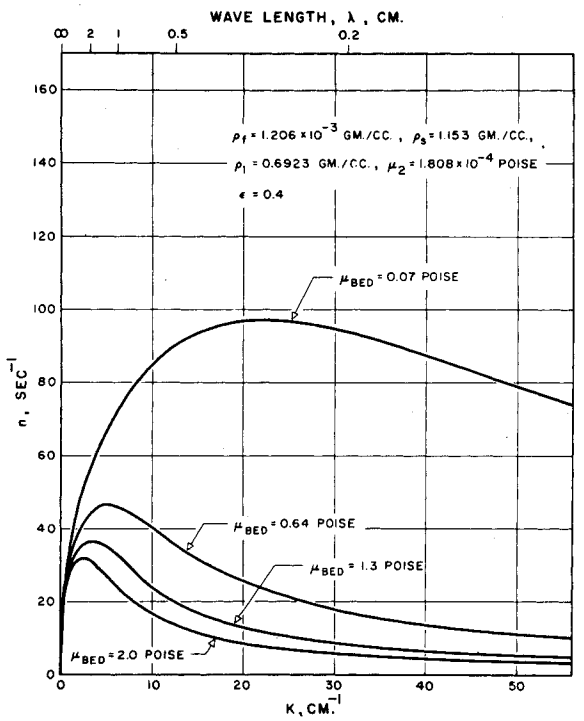

Fig. 5. Effect of bed phase viscosity for model 2 system: Aerocat catalyst-air, unstable interface.

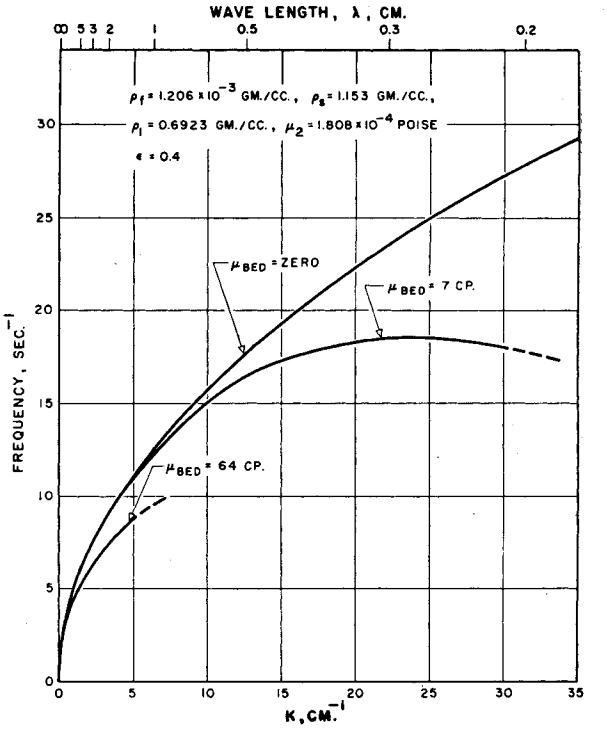

Fig. 6. Effect of bed phase viscosity for model 2 system: Aerocat catalyst-air, stable interface.

that disturbances of wave lengths corresponding to maximum n will outgrow others and predominate, given a spectrum of disturbances. Thus, as noted in Figure 5, low-viscosity beds would favor destruction of the oversize bubble with instabilities on its upper surface leading to smaller entities than would beds of high viscosity. For the three high-viscosity beds in the figure the maximum n occurs for wave lengths in the order of 1 to 2 cm. For the low bed viscosity of 7 centipoises this maximum occurs near a wave length of 0.3 cm. Bubbles larger than 0.3 cm. would be liable to destruction for the latter case; whereas only those larger than 1 or 2 cm. would be liable to destruction for the former. In other words beds of high viscosity would tend to form and maintain larger bubbles than would beds of low viscosity, thus tending toward poorer quality of fluidization. These conclusions are consistent with the reported findings of Matheson, Herbst, and Holt (*5*).

Stable Interface

Figure 6 illustrates typical relations between n and K for the stable (upper bed) interface by using model 2, selected because it includes bed viscosity as a variable. Roots of n at stable interfaces consist of a complex conjugate pair, the negative real part corresponding to damping of amplitude and the imaginary part to oscillation frequency of the wave. Frequency of the damped wave $(I(n)/2\pi)$ has been plotted vs. K. For comparison Taylor's equation (*8*) for nonviscous fluids

$$\left\{n = +\sqrt{\frac{[-gK(\rho_1 - \rho_2)]}{[\rho_1 + \rho_2]}}\right\}$$

also is represented. In Table 2 there are assembled all roots for the system properties represented in Figure 6.

Table 2. Roots of n For the Stable Interface (Model 2)

System: Aerocat catalyst–air; ϵ = 0.4, ρ_s = 1.153 g./cc., ρ_f = 1.206 × 10^{-3} g./cc., μ_2 = 1.808 × 10^{-4} poise

K, cm.$^{-1}$	μ_1, centipoises	n, sec.$^{-1}$ Taylor equation	n, sec.$^{-1}$ Equation (34)
5	7	± 70i	− 4.44 ± 69.1i
10	7	± 99i	− 15.4 ± 94.6i
20	7	±140i	− 46.1 ± 115.0i
30	7	±171i	− 74.6 ± 113.2i
2	64	± 44.2i	− 5.84 ± 42.9i
5	64	± 70i	−24.73 ± 54.9i

As wave length becomes larger, that is as the wave number approaches zero, damping and frequency both approach zero; thus long waves have a low frequency of oscillation and very little damping, while very short waves are damped rapidly. However, because of the maximum in the frequency–vs.–wave-number relation given in Figure 6, frequency of oscillation tends toward small values at both large and small wave lengths. As bed viscosity is taken to approach zero, the frequency component approaches parabolic form (Taylor equation); that is, the maximum goes to very high wave numbers. In this limit there is, of course, no damping of an imposed wave.

Figure 6 shows also that bed viscosity is a significant variable in its effect on the wave characteristics of inherently stable upper interfaces of fluidized beds. However possibility of discrimination between frequency values in beds of different viscosities tends to disappear at small wave numbers (large wave lengths). The frequency–wave-number relationships suggest experiments for measuring bed viscosity based upon these relationships and avoiding the necessity of inserting substantial obstructions in the bed, as is customary in some methods. When one assumes that support fluid and particle properties as well as fraction voids are obtainable, viscosity measurements would entail determination of wave lengths for oscillations at a series of definite frequencies produced in the upper surface by means of paddles or similar devices. Actually only one frequency would be needed if the bed phase were a Newtonian fluid, but the use of several different frequencies allows the evaluation of the viscosity for the actual non-Newtonian bed phase.

Solutions of the linearized Navier-Stokes equations presented here relate to the behavior of fluidized-bed interfaces and not to the interior of such beds. However the techniques developed by Morse (*6*), Grohse (*2*), and others for determining the quality of fluidization by the capacitance of some region in the bed or the absorption of X-rays along some path through the bed relate directly

to the quality of fluidization within the bed. Nevertheless the indirect approach to the quality of fluidization by stability analysis of the bed interface yields results which show the same dependence on bed properties as the direct approach. The correspondence is not quite perfect, perhaps because full development of bubbles or similar discontinuities involves the nonlinear terms which relate velocity to the rate of change of velocity. Nonlinearities may also be essential in describing bubble interactions, as have been suggested to occur in vortex interaction in the classic fluid mechanical transition problem. However, despite nonlinear effects, empirical relations between the quality of fluidization and the methods of analysis in this paper may be possible.

ACKNOWLEDGMENT

The authors wish to express their appreciation to the Shell Development Company, Emeryville, California, for support of this investigation through an education-research grant. The assistance of Robert Goerss in programing and machine computation in connection with the extraction of roots is acknowledged with thanks.

NOTATION

d = particle diameter, cm.
g = acceleration of gravity, cm./sec.^{2}
i = $\sqrt{-1}$
m = parameter $= +\sqrt{K^2 + \frac{\rho n}{\mu}}$
n = reciprocal time constant, sec.$^{-1}$
p = pressure, g. (mass)/(sec.^{2})(cm.)
t = time, sec.
u = local velocity in x direction
v = local velocity in y direction
x = direction along axis of wave, horizontal
y = direction perpendicular to axis of wave, vertical
A, B, C, C_1, D = constants
C' = slip velocity of interface referred to support-fluid phase, a function of the system and ϵ; positive direction is upward
F = body force on fluid per unit mass of fluid due to particle friction
G = function defined in Equation (36)
H = function defined in Equation (37)
$I(n)$ = coefficient of imaginary part of n
K = wave number $= 2\pi/\lambda$
M, N = slip velocity of particles with reference to support fluid in dense bed phase and support fluid phase respectively

Greek Letters

ϵ = fraction voids in bed
η = interface position
λ = wave length
μ = viscosity
ρ = density
ϕ, ψ = potential functions

Subscripts

0 = at time zero
0_1 = at interface on bed side
0_2 = at interface on support fluid side
1 = dense bed phase or time one
2 = support fluid phase or time two
b = actual bed value
f = support fluid
v = virtual ($\rho_v = \rho_s + \frac{1}{2}\rho_f$)
s = solid particle
x = in x direction
y = in y direction

LITERATURE CITED

1. Bellman, Richard, and R. H. Pennington, *Quart. Appl. Math.*, **12**, 151 (1954).
2. Grohse, E. W., *A.I.Ch.E. Journal*, **1**, 358 (1955).
3. Lewis, D. J., *Proc. Roy. Soc.*, (*London*), **A202**, 81 (1950).
4. Long, F. J., M.S. thesis, Princeton University, Princeton, New Jersey, (May, 1952).
5. Matheson, G. L., W. A. Herbst, and P. H. Holt, 2nd, *Ind. Eng. Chem.*, **41**, 1099 (1949).
6. Morse, R. D. and C. O. Ballou, *Chem. Eng. Progr.*, **47**, 199 (1951).
7. Rice, W. J., Ph.D. dissertation, Princeton University, Princeton, New Jersey (1959).
8. Taylor, G. I., *Proc. Roy. Soc.*, (*London*), **A201**, 192 (1950).
9. Wilhelm, R. H. and Mooson Kwauk, *Chem. Eng. Progr.*, **44**, 201 (1948).

APPENDIX

The linearized equations of motions (2) and (3) for the Taylor type of analysis used earlier in this paper do not permit the explicit introduction of the effect of slip velocity between particles and support fluid upon the behavior of the bed interface. A modified procedure suggested by analyses of flame fronts of Landau (*A1*) and Markstein (*A2*) overcomes this difficulty at the expense of satisfying one less condition at the interface between the bed and support fluid. This appendix compares conclusions from the Taylor and Landau types of stability analyses.

The models of beds utilized are the same as were used previously. Linearized equations of continuity and motion are written and applied to an interface initially sinusoidally disturbed as before. An outline of the derivation for the lower bed interface of a model 2 bed follows. (Complete details of derivation are available in reference 7.)

The local horizontal velocity at any point is given by

$$u = U + u' \tag{39}$$

the local vertical velocity by

$$v = V + v' \tag{40}$$

and the pressure by

$$p = P + p' \tag{41}$$

(By comparison the Taylor type of analysis dealt only with the composite u, v, and p.)

Equation of Continuity

$$\frac{\partial u'}{\partial x} + \frac{\partial v'}{\partial y} = 0 \tag{42}$$

Equations of Motion

$$\frac{\partial u'}{\partial t} + V\frac{\partial u'}{\partial y} = -\frac{1}{\rho}\frac{\partial p'}{\partial y} + \frac{\mu}{\rho}\left(\frac{\partial^2 u'}{\partial x^2} + \frac{\partial^2 u'}{\partial y^2}\right) \tag{43}$$

$$\frac{\partial v'}{\partial t} + V\frac{\partial v'}{\partial y} = -\frac{1}{\rho}\frac{\partial p'}{\partial x} + \frac{\mu}{\rho}\left(\frac{\partial^2 v'}{\partial x^2} + \frac{\partial^2 v'}{\partial y^2}\right) \tag{44}$$

It may be noted in passing that the Landau type of formulation leads to the retention, after linearization, of the second, that is, the convective, term in each of the equations of motion, whereas this term disappears in the Taylor type of formulation [Equations (2) and (3)].

Potential functions ϕ and ψ are now defined as

$$u' = -\frac{\partial \phi}{\partial x} - \frac{\partial \psi}{\partial y} \tag{45}$$

$$v' = -\frac{\partial \phi}{\partial y} + \frac{\partial \psi}{\partial x} \tag{46}$$

$$p' = \rho\frac{\partial \phi}{\partial t} \tag{47}$$

with the restrictions

$$\frac{\partial^2 \phi}{\partial x^2} + \frac{\partial^2 \phi}{\partial y^2} = 0 \tag{48}$$

$$\frac{\partial \psi}{\partial t} + V\left(\frac{\partial \phi}{\partial x} + \frac{\partial \psi}{\partial y}\right) = \frac{\mu}{\rho}\left(\frac{\partial^2 \psi}{\partial x^2} + \frac{\partial^2 \psi}{\partial y^2}\right) \tag{49}$$

To satisfy these equations for the bed phase a solution is written in the following equations:

$$\phi_1 = Ae^{-Ky+nt}\cos Kx \tag{50}$$

$$\psi_1 = Be^{-m_1 y+nt}\sin Kx - \frac{KV_1 A}{(KV_1 - n)}e^{-Ky+nt}\sin Kx \tag{51}$$

$$p_1' = \rho_1\frac{\partial \phi_1}{\partial t} \tag{52}$$

where m_1, which must be positive, is given by

$$n = V_1 m_1 + \frac{\mu_1}{\rho_1}(m_1^2 - K^2) \tag{53}$$

For the support-fluid phase (the lower phase) these equations provide a solution:

$$\phi_2 = Ce^{Ky+nt} \cos Kx \tag{54}$$

$$\psi_2 = \frac{V_2KC}{V_2K + n} e^{Ky+nt} \sin Kx \tag{55}$$

$$p_2' = \rho_2 \frac{\partial \phi_2}{\partial t} \tag{56}$$

The interfacial position may be given by $\eta(x, t)$. Then

$$\frac{\partial \eta}{\partial t} = v_2' = -\frac{\partial \phi_2}{\partial y} + \frac{\partial \psi_2}{\partial x}$$

$$= \frac{-KnC}{V_2K + n} e^{Ky+nt} \cos Kx \tag{57}$$

Hence on integration

$$\eta = \frac{-KC}{V_2K + n} e^{Ky+nt} \cos Kx \tag{58}$$

When one takes

$$\eta_0 = \frac{-KC}{V_2K + n} e^{Ky} \cos Kx \tag{59}$$

then

$$\frac{\eta}{\eta_0} = e^{nt} \quad \text{at any} \quad x \tag{60}$$

To relate the constant n to the wave length of the surface disturbance, the physical properties of the fluid phases, and the slip velocity between particles and support fluid, the following interfacial boundary conditions are imposed:

$$u_1' + V_1 \frac{\partial \eta}{\partial x} = u_2' + V_2 \frac{\partial \eta}{\partial x} \tag{61}$$

$$v_1' = v_2' \tag{62}$$

$$-gy(\rho_1 - \rho_2) + p_1' - 2\mu_1 \frac{\partial v_1'}{\partial y}$$

$$= p_2' - 2\mu_2 \frac{\partial v_2'}{\partial y} \tag{63}$$

Since only three conditions can be satisfied at the interface, the choice of the preceding three is dictated by the need to find solutions which degenerate to other previously known limiting solutions. The condition which has been discarded is the equality of the shear stresses on either side of the interface.

By substitution from Equation (45) to (47), (50) to (52), (54) to (56), and (58) into (61) to (63), the following final solution relating n to K and the other physical properties is obtained for model 2

$$g(\rho_1 - \rho_2)K + \rho_1K^2V_1(V_1 - V_2)$$

$$+ \mu_1K^2(V_1 - V_2)(m_1 - K)$$

$$+ nK(-2\mu_2K - \rho_2V_2 - \rho_1V_1$$

$$- 2\mu_1m_1) - n^2(\rho_1 + \rho_2) = 0 \tag{64}$$

Similarly for model 1 the final solution is

$$gK(1 - \epsilon)(\rho_s - \rho_f) + \rho_fK^2V_1^2(1 - \epsilon)$$

$$+ \mu_fK^2V_1(1 - \epsilon)(m_1 - K)$$

$$+ nK[-2\mu_f(K + m_1) - \rho_fV_1(1 + \epsilon)]$$

$$- 2\rho_fn^2 = 0 \tag{65}$$

Equation (65) is identical with Equation (29) when $V_1 = 0$.

These solutions apply to the lower bed interface, which is unstable; similar equations for the stable, upper bed interface may be obtained in a similar fashion.

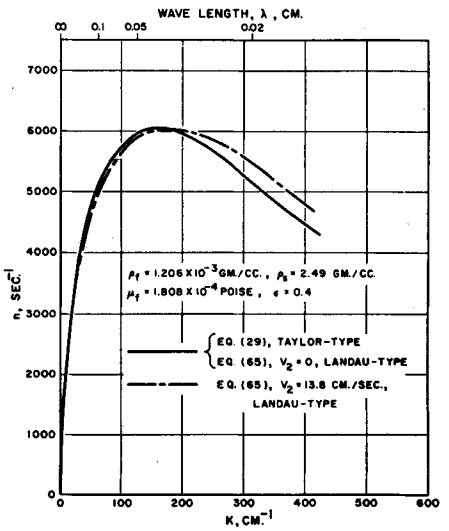

Fig. 7. Comparison of formulations for model-1 system: glass-air, unstable interface for different slip velocities (V_2).

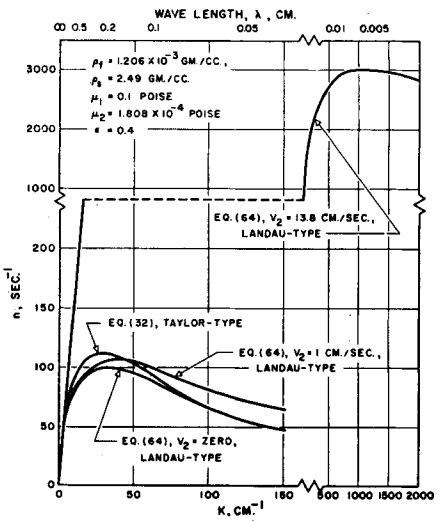

Fig. 8. Comparison of formulations for model-2 system: glass-air, unstable interface for different slip velocities (V_2).

Figures 7 and 8 show results of some calculations based on Equations (64) and (65) for fluidization of glass beads in air. Figure 7 compares n vs. K curves for the Taylor type of analysis stemming from Equation (29) with the Landau type, Equation (65), both for model 1. The slip velocity chosen for computation was 13.8 cm./sec. based on the empty column and corresponding to a velocity somewhat greater than the minimum fluidizing velocity for No. 7 glass beads (diameter = 0.0201 in. or 0.051 cm.), which is 9.15 cm./sec. (9). Even at this rather high slip velocity the difference between the results of the two approaches is very small, the major difference being a slight decrease in n at low K and a slight increase at higher values of K. As previously mentioned, Equation (65) becomes identical with Equation (29) when the slip velocity is zero.

Thus for model 1 in the range of slip velocities encompassing likely fluid-bed behavior the effect of this variable is noted to be small, as indicated by the small difference in the value of n calculated by the two approaches.

Comparisons for model 2 for the results of computations according to the two formulations in question are provided in Figure 8. As a result the following statements may be made:

1. At zero slip velocity ($V_2 = 0$) the Taylor and Landau types of formulations lead to closely similar curve shapes with small vertical displacement between them.

2. In the Landau type of formulation the presence of increasing slip velocities leads to substantial increases in instability, with curve maxima being shifted to increasing values of K. However at the largest value of slip velocity depicted ($V_2 = 13.8$ cm./sec.), the assumptions inherent in model 2 (that is, an emulsion with small slip velocity) became strained and might be considered inconsistent with the model. Thus, as in the case of model 1, model 2 may be concluded (for slip velocities consistent with the model) to be equally well described by the two modes of formulation.

In conclusion the two ways of writing the equations of motion yield results which are very nearly the same for commonly occurring physical situations.

NOTATION

p' = transient pressure component
u' = horizontal transient velocity component
v' = vertical transient velocity component
P = steady state pressure component
U = horizontal steady state velocity component
V = vertical steady state velocity component

LITERATURE CITED

A1. Landau, L., *Acta Physicochim. U.R.S.S.*, 19, 77 (1944).
A2. Markstein, G. H., *J. Aeronaut. Sci.*, 18, 199 (1951).

Presented at A.I.Ch.E. Chicago meeting. Manuscript received November 29, 1957; revision received April 3, 1958; manuscript accepted April 7, 1958.